

Effect of nitrogen injection time on structural and mechanical properties of AlN particles in aluminum matrix composite by *in-situ* gas bubbling method

Nguyen Quoc Tuan^{1,*}, Duong Van Thiet¹, Nguyen Tien Tung¹, Pham Van Dong²

¹*Faculty of Mechanical Engineering, Hanoi University of Industry, No. 298, Cau Dien street, Bac Tu Liem District, Ha Noi, Viet Nam*

²*Department of Science and Technology, Hanoi University of Industry, No. 298, Cau Dien street, Bac Tu Liem District, Ha Noi, Viet Nam*

*Email: tuannq@hau.edu.vn

Received: 7 July 2023; Accepted for publication: 11 March 2025

Abstract. In this paper, we report on the effect of nitrogen injection time on formation of AlN crystal particles in aluminum matrix by *in-situ* gas-bubbling method. The magnesium content with 15 wt.% was added into Al matrix as a catalyst. The results show that AlN polycrystalline particles were formed with hexagonal structures, featuring lattice constants $c = 4.969 \text{ \AA}$ and $a = 3.107 \text{ \AA}$. The crystallite size was decreased as increased nitrogen injection time, while the AlN particles density and micro-hardness were increased. The SEM images indicated that the AlN particles size varies from a few hundred nm to several μm . The micro-hardness testing was conducted using ISOSCAN HV2 AC instrument, and the highest value of sample obtained was 120 HV at nitrogen injection of 4 hours. The fabrication of AlN/Al composite using the *in-situ* gas-bubbling method is still a potential application for manufacturing industrial large scale.

Keywords: aluminum nitride; *in-situ* methods, metal composite, microstructure, gas injection, mechanical properties.

Classification numbers: 2.5.1, 2.9.1, 2.9.4.

1. INTRODUCTION

In recent years, aluminum composite materials include reinforcement particles have been significantly attracting because it possesses unique physical, chemical and mechanical properties. Therefore, it has potential applications in the automotive, aerospace and defense industries [1]. Among them, the AlN/Al composite has superior properties compared to other aluminum composites because the AlN material has special properties: It crystallizes in the hexagonal wurtzite structure with lattice constants $a = 3.110 \text{ \AA}$, $c = 4.980 \text{ \AA}$ [2]. It has a large band gap of 6.3 eV that makes it a good insulating material. It has a low density (3.026 g/cm^3), a low coefficient of thermal expansion ($4.5 \times 10^{-6} \text{ K}^{-1}$, in the temperature range 293 - 673 K and a very good thermal conductivity ($110 - 285 \text{ W m}^{-1} \text{ K}^{-1}$), high electrical resistance ($10^9 - 10^{11} \Omega\text{m}$), high Young's modulus ($E = 348 \text{ GPa}$), high compressive strength (2700 MPa) and

hardness (12.6 GPa), good thermal stability (up to 2000 K) [3 - 4]. The AlN/Al composites were still studying by two methods: *ex-situ* and *in-situ* [3 - 23]. The technologically advanced features of the *in-situ* method compared to the *ex-situ* are such as: i) the AlN reinforcement particles were formed during reaction processing, which enhanced the bondability of the reinforced particles to Al matrix; ii) the formation of AlN reinforcement particles is more uniform; iii) the production cost of AlN/Al composite is cheaper than by other methods since the technological generation of AlN powder is still a difficult problem. The *in-situ* gas-bubbling method is still a potential fabrication method. Although the knowledge of this method was studied quite early [3, 6, 10 - 15] but to have optimal technology with mechanical properties, and physical-chemical properties there is still a problem. Kumari *et al.* reported on the influence of nitrogen injection time, the role of magnesium on the formation of AlN particles and AlN/Al composition's micro-hardness. The results indicated that the hardness increases as the injection time increases, and the role of magnesium in composites generated AlN formation more fastly, thereby improving the composite's hardness [3]. Zheng *et al.* showed that the rate of formation of AlN increased slightly with the increase in the reaction temperature and increased significantly when the increase in gas flow rate, and kind of gaseous precursor when using NH_3 gas will generate AlN formation more than compared to using N_2 [6, 10]. Pradhan *et al.* reported that the AlN/Al composites were made using a mixture of $\text{NH}_4\text{Cl} + \text{CaO}$ to produce NH_3 gas that have the role as gas-bubbling to form AlN, resulting in composites with a hardness of 61.3 HV [5].

In this paper, we investigated the influence of nitrogen injection time on the structural and mechanical properties of AlN/Al composites using the *in-situ* gas-bubbling method. The structural properties will be discussed through the results of X-ray diffraction (XRD), scanning electron microscopy (SEM), and energy dispersive X-ray (EDX). Micro-hardness was investigated using ISOSCAN HV2 AC equipment.

2. MATERIALS AND METHODS

The experimental procedure was reported in our previous publication [14, 15]. The process details can be described as the following: Firstly the aluminum raw material and experiment tools were dried at 100 °C to clean organic contamination. Next step, 1 kg of Al-15 wt.% Mg was melted at 680 °C. After degassing, refined 0.35 kg Al-Mg alloy was poured into Al_2O_3 crucible and put in the reaction chamber. Raising temperature inside reaction chamber until achieved 1150 °C, the nitrogen injection processing began at a rate of 0.2 liters/minute, which was monitored by a flow meter. Before injecting nitrogen gas into reaction chamber, the gas was passed through a drying, dehumidification and deoxidation equipment. Before closing the furnace, Ar gas was introduced to protect the Al-Mg alloy liquid and prevent oxidizing or burning of Mg. The reaction chamber was sealed and protected by Ar gas to facilitate the favorable formation AlN. The variable injection times changed from 1 to 4 hours. The samples in the experiment are labeled as S1, S2, S3, and S4, corresponding to the nitrogen injection times as shown in Table 1. After injection time finished, the crucible was taken out from the furnace chamber and poured into the mold with size of 20 mm diameter. The sample was cut into specimens for structural and hardness characterization. The crystal structure was characterized by X-ray diffractometer EQUINOX 5000 Thermo Scientific (France) with Cu-K_α radiation, $\lambda = 1.54056 \text{ \AA}$. The lattice parameters were determined using Si as a standard deviation ($\pm 0.002 \text{ \AA}$). The composition of the sample was determined by EDX with standard deviation ($\pm 5 \%$), surfaces morphology were characterized using scanning electron microscope SEM-SU3800. The ISOSCAN HV2 AC with standard deviation ($\pm 0.025 \text{ HV}$) was used to determine the microhardness (Vickers Hardness Number, VHN) at different test loads of 0.25,

0.5, 1 and 2 N, dwell time of 13 s. The average values of 4 - 5 readings were taken as a measure of the representative hardness of the AlN/Al composite.

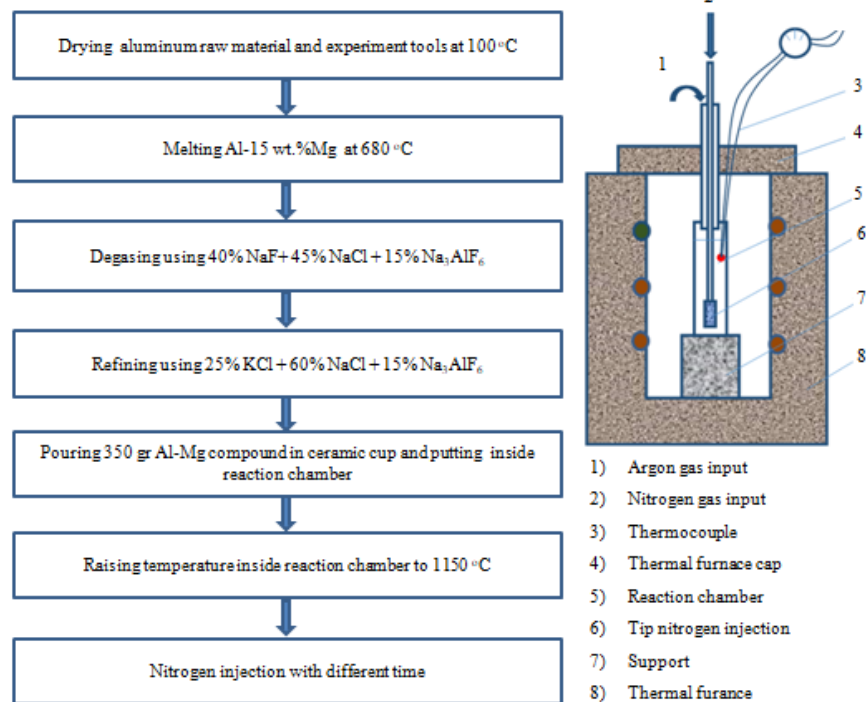


Figure 1. Experimental procedure and schematic illustration of reaction furnace for fabricating AlN/Al composite.

Table 1. Sample fabrication conditions with variable injection times.

Sample	Gas injection rate (liter/min.)	Injection time (hour)	Reaction chamber condition
S1	0.2	1	sealed
S2	0.2	2	sealed
S3	0.2	3	sealed
S4	0.2	4	sealed

3. RESULTS AND DISCUSSION

3.1. XRD results of AlN/Al composites

Figure 2 shows the X-ray diffraction patterns of samples with different blow times. There are three phases in all samples, as shown in Figure 2a): Al, Al-Mg, and AlN. Al phase marked by green color symbol, Al-Mg phase by square dot and AlN phase by black color symbol. The presence of Al-Mg phase in the sample may indicate that the injection time is not long enough for the whole reacting of Mg content in Al-Mg composite. In this case magnesium acts as catalysts to prevent aluminum oxidation reactions. Borgonovo *et al.* indicated that magnesium reacted to oxygen easier than aluminum [24]. Hou *et al.* showed the role of Mg to act as an

intermediate in the reaction between the nitrogen gas phase and the aluminum liquid phase to form AlN [8]. The samples S1, S2 with shorter nitrogen injection times, exhibited a more pronounced appearance of the Al-Mg phase with higher diffraction peaks. Kumari *et al.* reported that the content of 4 wt.% Mg added into Al matrix during nitrogen blowing time of 4 hours without the appearance of Al-Mg phase [3]. Dyzia *et al.* reported that the content of 3 wt.% Mg added into Al matrix after an hour nitrogen blow time without Al-Mg phase [7]. Shin *et al.* reported that 10 and 20 wt.% of Mg amounts were added into Al matrix, after the reaction time of 16, 32 hours respectively, there are no appearance of the Al-Mg phase [13]. The appearance of the AlN structural phase significantly shows on sample S4 as in Figure 2b), with the diffraction angles at 33.3°, 36.1° and 38.0° corresponding to the diffraction plane (100), (002) and (101). Comparing, all of the received peaks of sample S4 to the diffraction peaks of the AlN bulk are matched to those of the standard card JCPDF#893446. The XRD results show that the AlN phase is polycrystalline and adopts a wurtzite hexagonal structure [25]. The lattice constant of hexagonal structure can be calculated following the formula:

$$\frac{1}{d_{hkl}^2} = \frac{4}{3} \left(\frac{h^2 + k + l^2}{a^2} \right) + \frac{l^2}{c^2} \quad (1)$$

where d_{hkl} is the distance between the diffraction planes and Bragg's law of diffraction with the angle of incidence of diffraction θ :

$$\lambda = 2d_{hkl} \sin \theta_{hkl}. \quad (2)$$

Based on formula (1) and (2) the lattice constants

$$a = \frac{\lambda}{\sqrt{3} \sin \theta_{(100)}}; \quad (3)$$

$$c = \frac{\lambda}{\sin \theta_{(002)}}. \quad (4)$$

The calculated a and c of AlN in this case were 3.107 and 4.969 Å, respectively. These values are quite consistent with previous reports [2, 25].

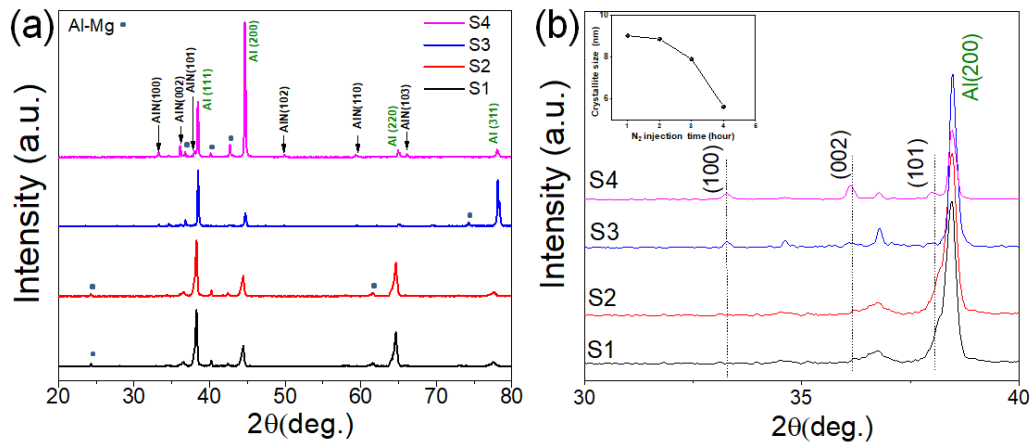


Figure 2.(a) X-ray diffraction pattern of AlN/Al at different N₂ blow times. (b) The enlarged patterns for the diffraction angle from 30 to 40 degree. The inset of (b) is crystallite size of AlN calculated at (101) peak.

The inset in Figure 2b) shows the AlN crystallite size calculated based on the diffraction peak (101). This value decreases as the blow time increases with the maximum crystallite size value of ~9 nm and the smallest value of ~5 nm. The crystallite size was calculated using the Debye Scherrer formula: $D = k\lambda/\beta\cos\theta$ [25], where D is the nanoparticles crystallite size, the k represents Scherrer constant, λ denotes the wavelength, β denotes the full width at half maximum (FWHM), the θ represent the Bragg angle. The obtained values of D are significantly lower than the reported crystal size of 46, 55 nm AlN in an AlN/Al composite fabricated by *ex-situ* method - ball milling during 20 hours [19].

3.2. The morphology of AlN/Al composite at various gas injection times

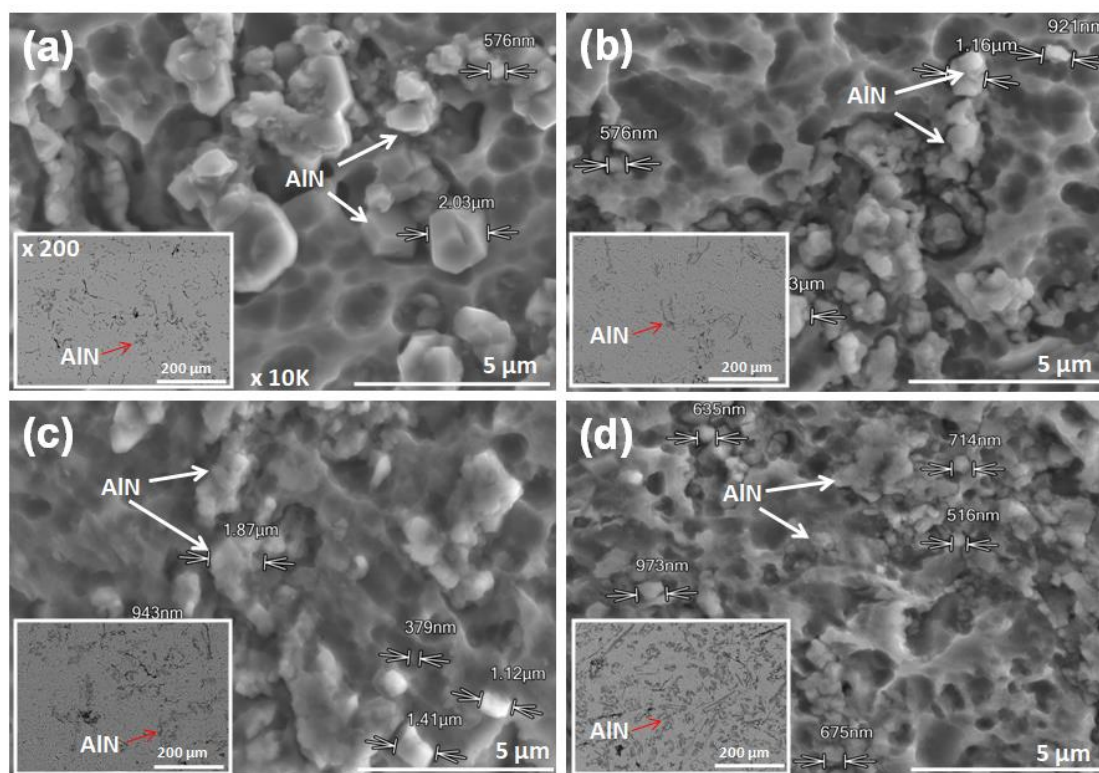


Figure 3. The SEM images of specimen with different N₂ injection times: (a)-S1, (b)-S2, (c)-S3, (d)-S4. The insets are SEM images with smaller magnification.

Figure 3 shows SEM image with the SE mode of AlN/Al composite's surface with different nitrogen injection times (a)-S1, (b)-S2, (c)-S3, (d)-S4. The samples possess particle sizes ranging from few hundred nm to several μm . The surface is free of pore and crack. With the same *in-situ* gas-bubbling method the previous reports showed particle sizes of less than 10 μm [11 - 13]. The AlN formation tends to agglomerate discontinuously into Al-Mg compound, which have the biggest particle size below 5 μm . The characteristic particle shapes are more exhibited in S1 sample with polygon shape. As the nitrogen injection time increased the particle density increased, distribution is more uniform and the particle size tends to be smaller. The inset image in Figures 3(a)-(d) shows SEM images with BSE mode at smaller magnification. Based on these images, the particle density of AlN formation increases. The distribution of AlN particles on sample S4 is fairly uniform in Al-Mg compound.

3.3. The composition of AlN/Al composite

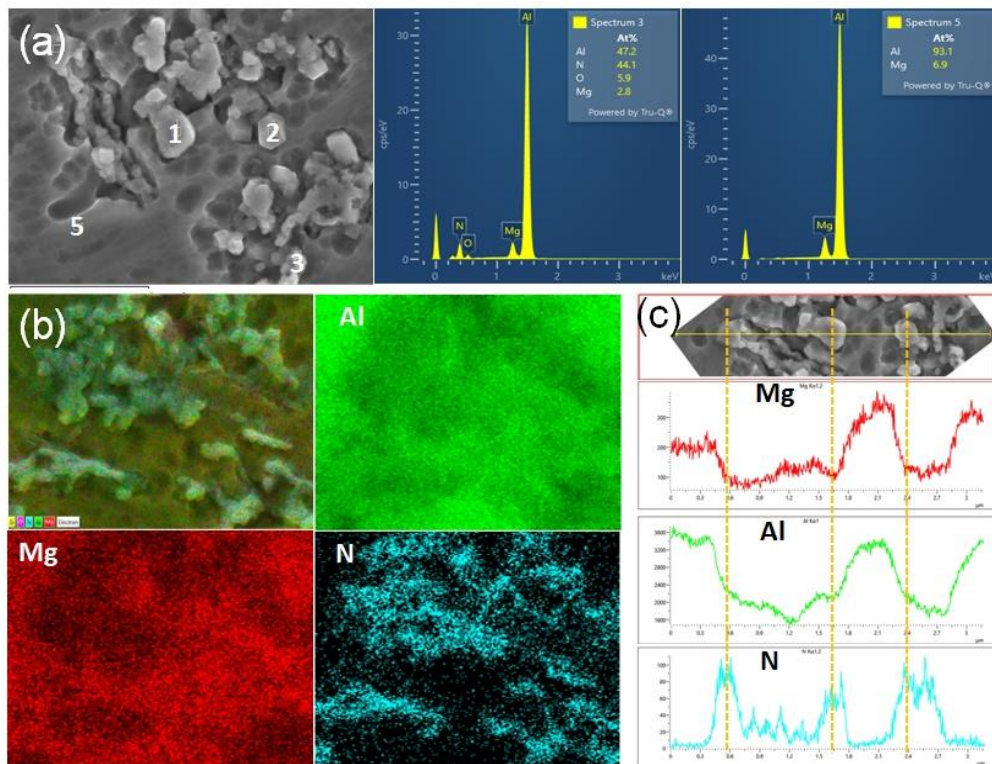


Figure 4. (a) The EDX point spectrum, (b) the EDX mapping, (c) EDX scan line of specimen with N_2 injection time of one hour.

Figure 4 shows the EDX point spectrum (a), EDX region spectrum (b), and EDX line spectrum (c) of sample S1. The Al/N atomic ratio of this sample was $47.2/44.1 = 1.07$, and those of samples S2, S3, and S4 were 0.97, 0.97 and 1.11, respectively. These results are quite consistent with the results of X-ray diffraction. The results in Figure 4(b-c) show more clearly the AlN particles formed on the Al-Mg compound.

3.4. Effects of micro-hardness property of AlN/Al composites

Figure 5(a) indicates the hardness value (HV) of some AlN/Al composites made by *in-situ* method and *ex-situ* method in recent years and Figure 5(b) is the micro-hardness value of samples with different nitrogen injection times compared to the hardness value of Al. The micro-hardness values were measured at different loads of 0.25, 0.5, 1 and 2 N by the Isoscan HV2 AC equipment. The results show that as injection time increases the hardness of the sample increases. This is due to the increased amount of AlN particle formation. Moreover, the crystallite particle size decreases to resist the deformation of the Al matrix, thereby increasing the hardness of AlN/Al composites. The hardness value of S4 sample is greater than 2.5 times than that of the pure Al. According to our previous report, the content of AlN particles during nitrogen injection time of 4 hours was about 6.32 % [14]. Kumari *et al.* measured a micro-hardness of 115 HV with a load of 0.25 N of AlN/Al composite with 4 wt.% Mg–Al during nitrogen injection time of 4 hours by *in-situ* gas–bubbling method [3]. Using the same measurement condition for S4 sample

the achieved microhardness was 98.4 HV. By *ex-situ* methods, the added AlN content is quite high [23, 26]. Liia *et al.* reported that with an AlN content of 70 wt.% in the AlN/Al composite, the hardness values measured with a load of 50 N were up to 145 HV [26]. Xiu *et al.* reported that an AlN content of 45 wt.% in the AlN/Al composite with a load of 250 N, the hardness values achieved at 127 HV [23]. The micro-hardness values in our samples were lower compared to those by *ex-situ* methods. This result may be due to the low AlN content in AlN/Al composite. However, based on this method the AlN/Al composites' hardness can be changed by controlling nitrogen injection time.

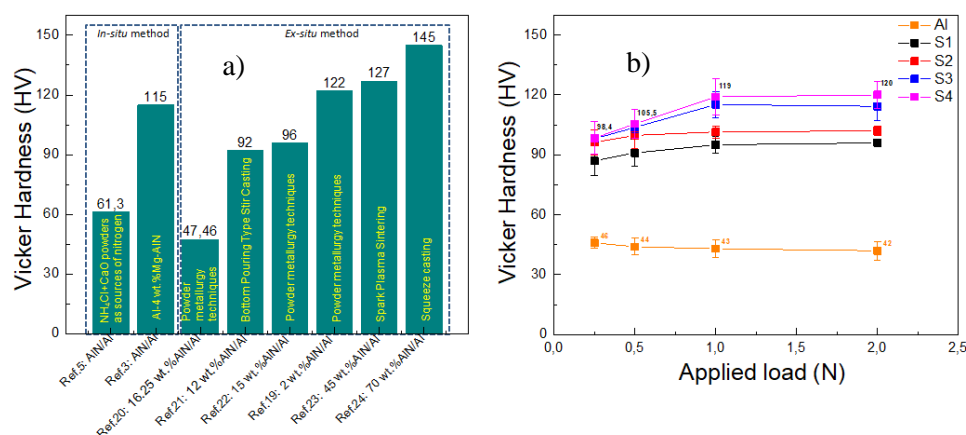


Figure 5.(a) The Vickers hardness of some AlN/Al composites fabricated by *in-situ* and *ex-situ* method. (b) The Vickers hardness of Aluminum and AlN/Al composite with different N₂ gas blow times.

4. CONCLUSION

In conclusion, in this paper we have analyzed the influence of nitrogen injection time on AlN particle formation in Al matrix. As a result, the formed AlN particles are polycrystalline with hexagonal structures. The density of AlN particles is uniform distribution on the Al-Mg compound with particle sizes ranging from a few hundred nm to several μm . The micro-hardness increases gradually with the nitrogen injection time and the maximum value of 120 HV is achieved when the sample is injected at 4 hours. By these results, the fabrication of AlN/Al composite using the *in-situ* gas-bubbling method is of great promising in industrial large scale.

Acknowledgement: The authors would like to acknowledge the financial support of Hanoi University of Industry under the Grant number of 04 – 2021 – RD/HĐ-ĐHCNHN. Authors are grateful for the support of experimental works by Materials Lab Center for Experimental Research and Precision Measurement of the Faculty of Mechanical Engineering, Hanoi University of Industry.

CRedit authorship contribution statement: Duong Van Thiet and Nguyen Tien Tung designed the experiments, performed some parts of the experiments, prepared figures; Pham Van Dong corrected the grammar of manuscript; Nguyen Quoc Tuan wrote and revised the manuscript.

Declaration of competing interest. The authors declare that they have no known competing financial interests or personal relationships that could have appeared to influence the work reported in this paper.

REFERENCES

1. Ujah C. O., Kallon D. V. V. - Trends in Aluminium Matrix Composite Development, Crystals 12 (10) (2022) 1357. <https://doi.org/10.3390/cryst12101357>

2. Schulz H., Thiemann K. H. - Crystal structure refinement of AlN and GaN, Solid State Commun. **23** (1977) 815-819. [https://doi.org/10.1016/0038-1098\(77\)90959-0](https://doi.org/10.1016/0038-1098(77)90959-0)
3. Kumari S. S. S., Pillai U. T. S., Pai B. C. - Synthesis and characterization of *in-situ* Al–AlN composite by nitrogen gas bubbling method, J. Alloys Compd. **509** (2011) 2503-2509. <https://doi.org/10.1016/j.jallcom.2010.11.065>
4. Balog M., Krizik P., Svec P., Orovčík L. - Industrially fabricated *in-situ* Al–AlN metal matrix composites (part A): Processing, thermal stability, and microstructure, J. Alloys Compd. **883** (2021) 160858. <https://doi.org/10.1016/j.jallcom.2021.160858>
5. Pradhan S., Jena S. K., Patnaik S. C., Swain P. K., and Majhi J. - Wear characteristics of Al–AlN composites produced *in-situ* by nitrogeneration, IOP Conf. Series: Materials Science and Engineering **75** (2015) 012034. <https://doi.org/10.1088/1757-99X/75/1/012034>
6. Zheng Q., Wu B., Reddy R. G. - *in-situ* Processing of Al Alloy Composites, Adv. Eng. Mater. **5** (2003) 167-172. <https://doi.org/10.1002/adem.200390027>
7. Dyzia M., Ślężiona J. - Aluminium matrix composites reinforced with AlN particles formed by *in-situ* reaction, Arch. Mater. Sci. Eng. **31** (2008) 17-20.
8. Hou Q., Mutharasan R., Koczak M. - Feasibility of aluminium nitride formation in aluminum alloys, Mater. Sci. Eng. A **195** (1995) 121-129. [https://doi.org/10.1016/0921-5093\(94\)06511-X](https://doi.org/10.1016/0921-5093(94)06511-X)
9. Adachi M., Hamaya S., Yamagata Y., Loach A. J., Fada J. S., Wilson L. G., French R. H., Carter J. L. W., Fukuyama H. - *in-situ* observation of AlN formation from Ni–Al solution using an electromagnetic levitation technique, J. Am. Ceram. Soc. **103** (2020) 2389-2398. <https://doi.org/10.1111/jace.16960>
10. Zheng Q., Reddy R. G. - Kinetics of *in-situ* Formation of AlN in Al Alloy Melts by Bubbling Ammonia Gas, Metall. Mater. Trans. B **34** (2003) 793-804. <https://doi.org/10.1007/s11663-003-0085-y>
11. Zheng Q., Reddy R. G. - Mechanism of *in-situ* formation of AlN in Al melt using nitrogen gas, J. Mater. Sci. **39** (2004) 141-149. <https://doi.org/10.1023/B:JMSC.0000007738.14116.fd>
12. Zheng Q., Reddy R. G. - Influence of Magnesium on Nitridation of Molten Aluminum from Nitrogen Bubbling Gas, High Temp. Mater. Process. **22** (2003) 63-71. <https://doi.org/10.1515/HTMP.2003.22.2.63>
13. Seon Shin K., Kim Y. S., Kim N. J. - CAAM Report 98001F, April 1998.
14. Hai N. H., Tuan N. Q. - Study on the Development of AlN Particles Synthesized by Gas/Liquid Reaction *in-situ*, Key Eng. Mater. **753** (2017) 71-77. <https://doi.org/10.4028/www.scientific.net/KEM.753.71>
15. Hai N. H., Tuan N. Q. - Analysis on the formation of AlN particles via gas/liquid reaction *in-situ*, Int. J. Emerg. Technol. Adv. Eng. **6** (11) (2016) 1-8.
16. Ma X., Zhao Y. F., Tian W. J., Qian Z., Chen H. W., Wu Y. Y., Liu X. F. - A novel Al matrix composite reinforced by nano-AlN_p network, Sci. Rep. **6** (2016) 34919. <https://doi.org/10.1038/srep34919>
17. Annapoorna T. L., Chandra B. T., Murthy S., Shivashankar H. S. - The study of sand abrasiveness behaviour of forged Al7075–AlN composites, Journal of Northeastern University **25** (2022) 1801-1813

18. Inoue A., Nosaki K., Kim B. G., Yamaguchi T., Masumoto T. - Mechanical strength of ultra-fine Al-AlN composites produced by a combined method of plasma-alloy reaction, spray deposition and hot pressing, *J. Mater. Sci.* **28**(1993) 4398-4404. <https://doi.org/10.1007/BF01154948>
19. Ghodsa H., Manafia S. A., Borhanib E. - Effect of Particle Size on the Structural and Mechanical Properties of Al-AlN Nanocomposites Fabricated by Mechanical Alloying, *Mech. Adv. Compos. Struct.* **2** (2015) 73-78. <https://doi.org/10.22075/mac.2015.394>
20. Polycarp E., Rahmat A., Derman M. N., Baba G. - Hardness and Wear properties of Al-AlN Composite Produced using Powder Metallurgy Route, *International Journal of Engineering Trends and Technology* **48** (2017) 161-166. <https://doi.org/10.14445/22315381/IJETT-V48P229>
21. Meignanamoorthy M., Mohanavel V., Velmurugan P., Ravichandran M., Wadi B. Alonazi, Sivakumar S., Atkilt Mulu Gebrekidan - Effect of Nanoaluminium Nitride Ceramic Particles on Microstructure, Mechanical Wear, and Machining Behavior of Al-Si-Mg Alloy Matrix Composites Produced by Bottom Pouring Type Stir Casting Route, *Journal of Nanomaterials* **2022** (2022) 1-14. <https://doi.org/10.1155/2022/5013914>
22. De Araujo E. R., De Souza M. M. S., Filho F. A., Gonzalez C. H., De Araujo Filho O. O. - Preparation of Metal Matrix Aluminum Alloys Composites Reinforced by Silicon Nitride and Aluminum Nitride Through Powder Metallurgy Techniques, *Materials Science Forum* **727-728** (2012) 259-262. <https://doi.org/10.4028/www.scientific.net/MSF.727-728.259>
23. Xiu Z., Ju B., Liu S., Song Y., Du J., Li Z., Zhou C., Yang W., Wu G. - Spark Plasma Sintering of AlN/Al Functionally Graded Materials, *Materials* **14** (2021) 4893, <https://doi.org/10.3390/ma14174893>
24. Borgonovo C., Makhoul M. M - Synthesis of Aluminum-Aluminum Nitride Nanocomposites by Gas-Liquid Reactions I. Thermodynamic and Kinetic Considerations, *Metall. Mater. Trans. A* **47** (2016) 5125-5135. <https://doi.org/10.1007/s11661-016-3665-6>
25. Alsaad A. M., Al-Bataineh Qais M., Qattan I. A., Ahmad Ahmad A., Ababneh A., Albataineh Zaid, Aljarrah Ihsan A. - Telfah Ahmad-Measurement and ab initio Investigation of Structural, Electronic, Optical, and Mechanical Properties of Sputtered Aluminum Nitride Thin Films, *Front. Phys.* **9** (2020) 115. <https://doi.org/10.3389/fphy.2020.00115>
26. Liia D. F., Huang J. L., Chang S. T. - The mechanical properties of AlN/Al composites manufactured by squeeze casting, *J. Eur. Ceram. Soc.* **22** (2002) 253-261. [https://doi.org/10.1016/S0955-2219\(01\)00255-2](https://doi.org/10.1016/S0955-2219(01)00255-2)